PAPER

Check for updates

Excited-state absorption for zinc phthalocyanine from linear-response time-dependent density functional theory

Chunrui Wang,[a] Junfeng Shao,[a] Fei Chen[a] and Xiaowei Sheng ✶[b]

The mechanism for zinc phthalocyanine (ZnPc) showing optical-limiting character is related to the first singlet excited-state absorption (ESA). Two distinct band peaks in this ESA spectrum (1.97 eV and 2.56 eV) were observed in experiments. However, the origin of the absorption is not well understood. In the present work, we perform accurate quantum mechanical calculations and analysis of the absorption of ZnPc in the first singlet excited state. It is found that the transitions of $S_1 \rightarrow S_3$ and $S_1 \rightarrow S_{24}$ are the origin of the first and second band peaks, respectively. Charge transfer character is observed between the edges and central parts of ZnPc for those two transitions, but occurs in opposite directions. It is gratifying to note that the absorption can be modified smoothly through the substitution of nitrogen atoms in ZnPc with methyne or benzene rings. The aggregation phenomenon is also investigated with ZnPc dimers. The present calculations show that the absorptions of two ZnPc molecules with cofacially stacked and slightly shifted cofacially stacked configurations both result in an obvious blueshift compared with the zinc phthalocyanine monomer. The present observations may be utilized in tuning the optical-limiting character of ZnPc.

I. Introduction

With the rapid development of intense light sources, more and more researchers have realized that designing materials for protecting light-sensitive materials is urgent.[1] Optical-limiting materials show a strong attenuation of light transmission at high input intensities but have a very high transmittance for light at low input intensities.[2–5] These materials can be used to protect light-sensitive materials from damage by high intensity light sources. Reversed saturation absorption (RSA) is one of the most important non-linear optical properties for materials showing optical-limiting character. The necessary condition for materials showing reversed saturation absorption properties is that the excited states have higher absorption compared with the ground state.[6] Therefore, investigations of the absorption spectra of the molecules in the ground (GSA) and excited states (ESA) are very important for the development of advanced optical limiters.

Organic compounds are potential candidates for optical-limiting materials, since those compounds generally show large and delocalized π-electron networks.[7–12]

Metallophthalocyanines as typical organic compounds have received lots of attention in this field.[6,13–19] Zinc phthalocyanine (ZnPc) as a metallophthalocyanine has attracted the greatest interest.[20–22] The absorption spectra of ZnPc in the ground state and excited states have been well studied in experiments. One of the most recent experimental measurements of the GSA and ESA was conducted by Savolainen *et al.*[13] They recorded the spectrally resolved pump–probe data of zinc phthalocyanine on time scales ranging from femtoseconds to nanoseconds. Two distinct bands peaking at 1.85 eV and 3.59 eV were observed in the GSA. In addition, it was found that the main bands of the first singlet excited state absorption are centered at 1.97 eV and 2.56 eV.

Theoretically, the absorption spectrum of ZnPc in the ground state has also been investigated extensively. Ricciardi *et al.* afforded an accurate description of the electronic spectrum of ZnPc in the ground state.[23] Theisen *et al.* studied the absorption spectra for seven derivatives of ZnPc in the ground state.[24] Yanagisawa *et al.* and Ueno *et al.* investigated the effect of molecularly stacked aggregation on the ground state absorption spectra.[25,26] However, theoretical investigation of the ESA for ZnPc has been less explored. This is mainly attributed to the fact that the developed quantum chemical methods to study ESA are limited and immature. As far as we know, the first and only theoretical prediction of the ESA for ZnPc was reported by Fischer *et al.*[6] They performed real-time time-dependent density functional theory (RT-TDDFT) calculations for ZnPc in the first singlet excited state.[6] The predicted band peaks overestimated

[a]State Key Laboratory of Laser Interaction with Matter, Changchun Institute of Optics, Fine Mechanics and Physics, Chinese Academy of Sciences, Changchun, 130033, China

[b]Anhui Province Key Laboratory of Optoelectric Materials Science and Technology, Anhui Laboratory of Molecule-Based Materials, The Key Laboratory of Functional Molecular Solids, Ministry of Education, Anhui Normal University, Wuhu 241000, Anhui, China. E-mail: xwsheng@mail.ahnu.edu.cn

Paper

the transition energies by 0.27 eV and 0.28 eV, respectively, compared with the experimental measurement. Although the spectral band of the ESA for ZnPc has been qualitatively predicted with the RT-TDDFT method, accurate quantum mechanical calculations and analysis of the absorption are still required to fully characterize the ESA.

Most recently, we found that the oscillator strengths for the transition between two excited states can be well described with the excited state wavefunctions approximated by a linear combination of singly excited configurations built from the Kohn–Sham orbitals. The computational cost of this method scales as N^4, which is much cheaper compared with the QR-TDDFT method.[27] This method was applied to ZnPc and it was shown that the predicted band peaks of ZnPc in the first singlet excited state are in excellent agreement with the experimental measurements.[27] According to this observation, we afford an accurate quantum mechanical analysis for the absorption of ZnPc in the first singlet excited state. The manuscript is organized as follows: the methods used to
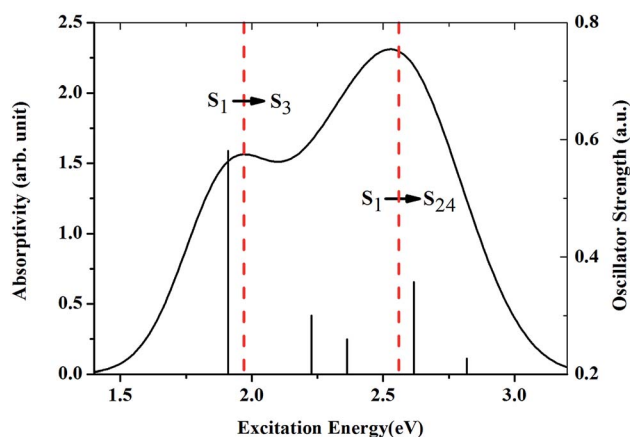

Fig. 2 Simulated absorption spectrum for ZnPc in the first singlet excited state (S_1), which is in good agreement with the experimental results. The red dashed lines are the two peaks of the spectrum observed in the experiment.
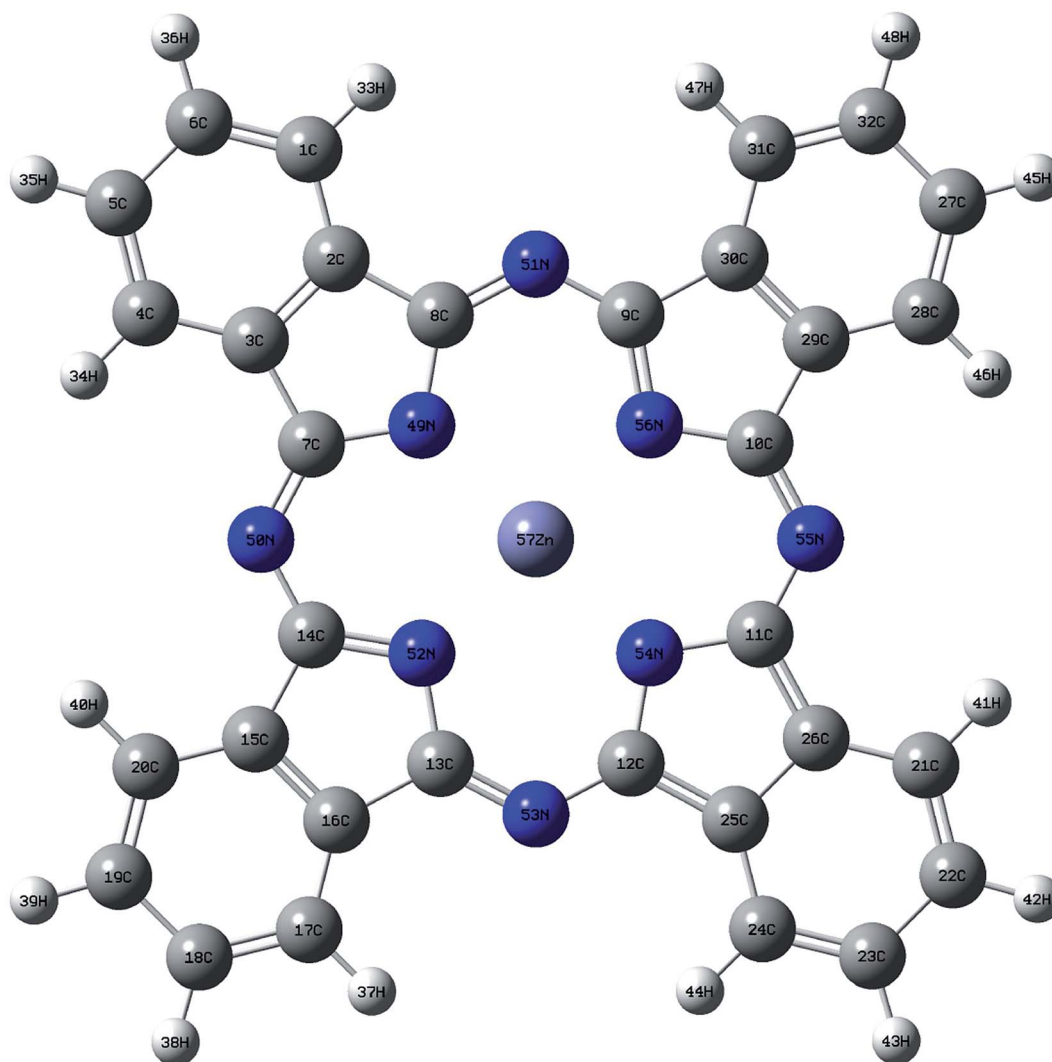

Fig. 1 Geometry of ZnPc optimized at BHandHLYP/6-31G(d,p) level in the ground state. White, grey and blue spheres represent hydrogen, carbon and nitrogen atoms, respectively.

estimate the ESA are described in the next section; the results are reported and discussed in the Results and discussions section; then, the paper closes with the Conclusions section.

II. Methods and computational details

The ESA of ZnPc, modified ZnPc and ZnPc dimers were simulated by using our recently proposed method. This method is

Table 1 The first five strong transitions of the theoretical ESA $S_1 \rightarrow S_n$

Transition	Excitation energy (eV)	Oscillator strength
$S_1 \rightarrow S_3$	1.9104	0.5806
$S_1 \rightarrow S_{10}$	2.2271	0.2998
$S_1 \rightarrow S_{13}$	2.3620	0.2594
$S_1 \rightarrow S_{24}$	2.6179	0.3569
$S_1 \rightarrow S_{27}$	2.8180	0.2263

based on the assumption that the excited state wavefunction can be well approximated by a linear combination of singly excited configurations built from the Kohn–Sham orbitals. The linear expansion coefficients are obtained by projecting the linear response orbitals on the Kohn–Sham orbitals. The transition energies are obtained from linear-response time-dependent density functional theory (LR-TDDFT). For validation and a more elaborate explanation of this method we refer to ref. 27.

The structure of the ground state ZnPc geometry was optimized with the BHandHLYP functional with the 6-31G(d,p) basis set. The basis set and the functional used here have been calibrated in ref. 27. The spectra are described using the calculated oscillator strengths and the excitation energies broadened with the Gaussian function (FWHM = 0.4 eV). The ESA simulations were done in DMSO solvent with the polarizable continuum model (PCM), which is consistent with the experimental measurements.[13] Geometry optimization was
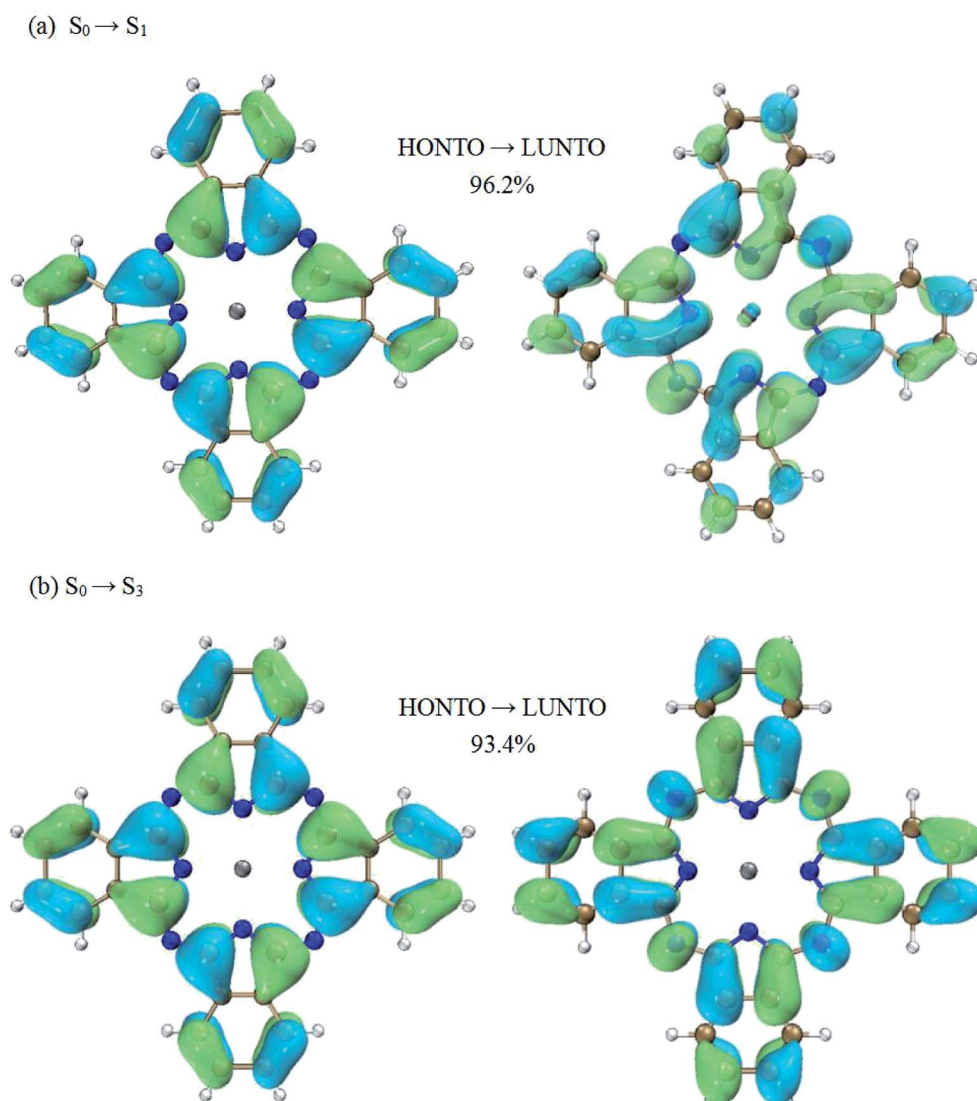

Fig. 3 Natural transition orbital analysis for the $S_0 \rightarrow S_1$ transition and $S_0 \rightarrow S_3$ transition. (a) $S_0 \rightarrow S_1$ transition: the weighting of this pair of NTOs (HONTO → LUNTO) is 96.2%. (b) $S_0 \rightarrow S_3$ transition: the weighting of this pair of NTOs (HONTO → LUNTO) is 93.4%.

done by using the Gaussian 09 package.[28] A modified GAME-SS(US) package was used to preform the LR-TDDFT and ESA simulations.[29] The natural transition orbital analysis and calculations of the electron density difference between the two singlet excited states were done using the wavefunction analysis program Multiwfn.[30]

III. Results and discussions

A. First singlet excited state absorption of ZnPc

The geometry of ZnPc is shown in Fig. 1. The calculated first singlet excited state absorption spectrum (black solid line) is shown in Fig. 2, together with the experimental results (red dashed lines).[13] The present theoretical predicted peak

positions of the ESA spectrum in Fig. 2 are 1.97 eV and 2.53 eV. Our calculations underestimate the transition energies by only 0.03 eV for the second peak, compared with the experimental measurement. We also note that Fischer *et al.* reported RT-TDDFT results for the present system.[6] The predicted two band peaks based on the RT-TDDFT calculations overestimated the transition energies by 0.27 eV and 0.28 eV, respectively, compared with the experimental measurement. More detailed discussions of the ESA calculated from RT-TDDFT can be found in ref. 31.

Table 1 lists the first five strong transitions of the theoretical prediction of ESA. It is clearly seen that $S_1 \rightarrow S_3$ is the main contribution to the first band peak. $S_1 \rightarrow S_{10}$, $S_1 \rightarrow S_{13}$, $S_1 \rightarrow S_{24}$ and $S_1 \rightarrow S_{27}$ all make considerable contributions to the second
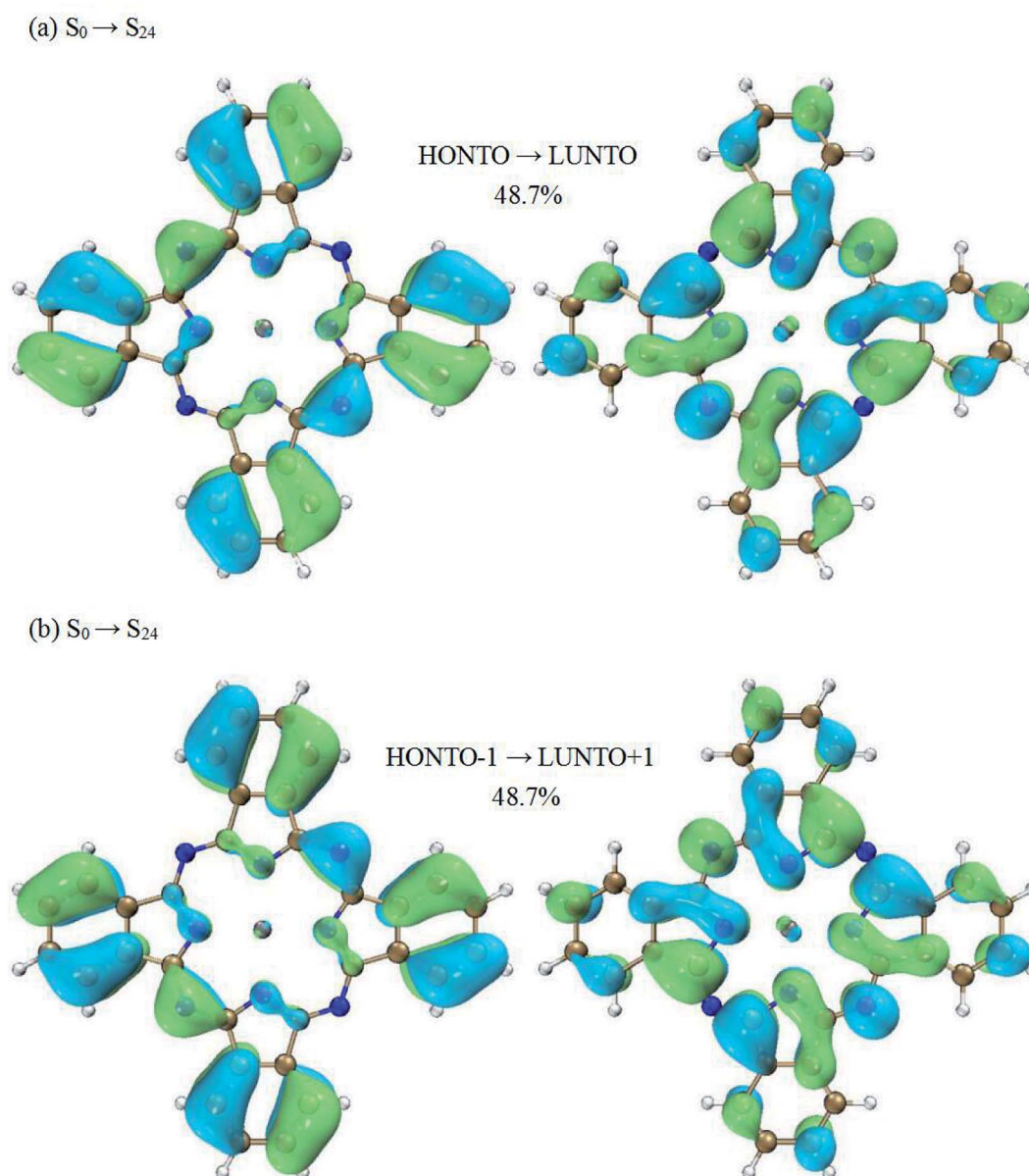

Fig. 4 Natural transition orbital analysis for the $S_0 \rightarrow S_{24}$ transition. (a) The weighting of this pair of NTOs (HONTO $\rightarrow$ LUNTO) is 48.7%. (b) The weighting of this pair of NTOs (HONTO$-1 \rightarrow$ LUNTO+1) is 48.7%.
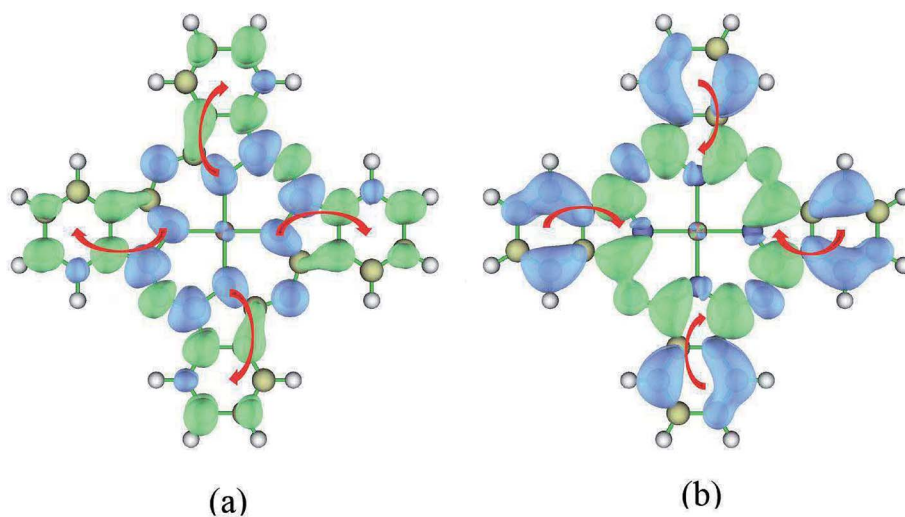
Fig. 5 Electron density difference of ZnPc for $S_1 \rightarrow S_3$ and $S_1 \rightarrow S_{24}$ transitions. Blue and green regions show a decrease and increase of electron density, respectively. The wavefunction analysis program Multiwfn[30] was used for this analysis. The isosurface values are fixed to 0.0005 Å^{-3}. (a) $S_1 \rightarrow S_3$, $\Delta\rho = \rho_3(r) - \rho_1(r)$; (b) $S_1 \rightarrow S_{24}$, $\Delta\rho = \rho_{24}(r) - \rho_1(r)$.
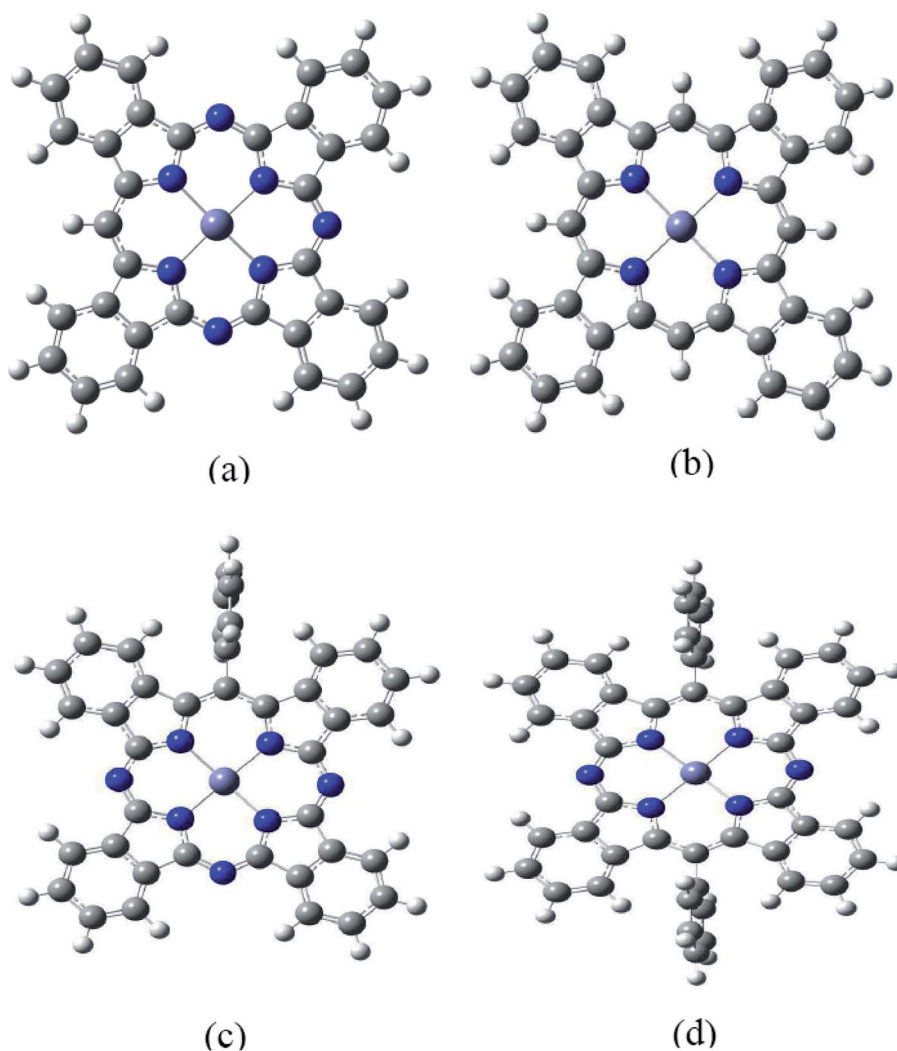

Fig. 6 Geometry of modified ZnPc optimized at the BHandHLYP/6-31G(d,p) level in the ground state. White, grey and blue spheres represent hydrogen, carbon and nitrogen atoms, respectively. (a) ZnTBTrAP, (b) ZnTBP, (c) ZnMPTBTrAP, (d) ZnTBtransDAP.

Paper

band peak. However, $S_1 \rightarrow S_{24}$ is the most important transition for the second peak in the ESA. Accordingly, S_1, S_3 and S_{24} are the excited states which are very important for the ESA. The orbital transitions for these key excited states in the ESA are also checked. It is found that S_1 essentially corresponds to the transition from the highest occupied to the lowest unoccupied molecular orbital (HOMO → LUMO). HOMO → LUMO+2 is the main transition for the excited state S_3. In the case of S_{24} the orbital transitions are complicated. Four transitions have to be included to describe this excited state (HOMO−5 → LUMO+1, HOMO−6 → LUMO, HOMO−6 → LUMO+1, HOMO−5 → LUMO).

Much insight can be gained from analyzing the charge transfer characters of the transitions between excited states. Firstly, let's focus on the transition of $S_1 \rightarrow S_3$, which is the dominant contribution to the first peak in terms of oscillator strength. According to the NTO analysis, the excited state of S_1 can be well characterized by a single electronic transition from the highest occupied natural transition orbital (HONTO) to the lowest unoccupied natural transition orbital (LUNTO) (96.2% HONTO → LUNTO). Similar results can also be observed for the excited state of S_3. The weighting of the HONTO → LUNTO transition for S_3 is 93.4%. These NTOs are shown in Fig. 3. It is shown that the transitions of $S_0 \rightarrow S_1$ and $S_0 \rightarrow S_3$ both present charge transfer character. For the $S_0 \rightarrow S_1$ transition, the charges move to the center part of ZnPc from the four benzene rings at the edges (Fig. 3(a)). For the $S_0 \rightarrow S_3$ transition, the charge transfer occurs in the opposite direction compared with the $S_0 \rightarrow S_1$ transition (Fig. 3(b)).

According to the above analysis for the transitions of $S_0 \rightarrow S_1$ and $S_0 \rightarrow S_3$, it is not hard to draw the conclusion that the $S_1 \rightarrow S_3$ transition has charge transfer character. To be specific, the charge transfer occurs from the center to the edges of ZnPc. This is also consistent with the calculations of electron density differences between the excited states of S_3 and S_1, as shown in Fig. 5(a).

Now we switch to the transition of $S_1 \rightarrow S_{24}$. This transition is the dominant contribution to the second peak. However, the excited state S_{24} cannot be characterized by a single electronic transition. Two electronic transitions have to be included based on the NTO analysis (HONTO → LUNTO and HONTO−1 → LUNTO+1). Fig. 4 displays the related NTOs. It is clearly shown that the $S_0 \rightarrow S_{24}$ transition has charge transfer character. The charge transfer occurs from the edges of ZnPc to the center part. Similar charge transfer character has been observed above for the transition of $S_0 \rightarrow S_1$. Therefore, it is not possible to judge the charge transfer character for the $S_1 \rightarrow S_{24}$ transition based on the NTO analysis for the transitions of $S_0 \rightarrow S_{24}$ and $S_0 \rightarrow S_1$. In order to clearly illustrate the charge transfer character of $S_1 \rightarrow S_{24}$, the electron density differences of ZnPc between the excited states of S_{24} and S_1 were also calculated. Fig. 5(b) displays the results and it can be seen that the charge transfer character also exists. However, the charge transfer occurs from the edges to the center part of ZnPc, which is in the opposite direction compared with the transition $S_1 \rightarrow S_3$. The charge transfer directions for the $S_1 \rightarrow S_3$ and $S_1 \rightarrow S_{24}$ transitions are shown in Fig. 5 by red arrows.

B. First singlet excited state absorption of modified ZnPc

It is well known that the optical properties of phthalocyanine-based materials can be tuned through chemical modifications.[24,32] Here we investigated four types of chemical modification for ZnPc (zinc tetrabenzotriazaporphyrin, ZnTBTrAP; zinc tetrabenzoporphyrin, ZnTBP; zinc monophenyltetrabenzotriazaporphyrin, ZnMPTBTrAP; zinc diphenyltetrabenzo*trans*diazaporphyrin, ZnDPTB*trans*DAP). These molecules were reported by Theisen *et al.*[24] A diagram of the modified ZnPc molecules is shown in Fig. 6. These chemical modifications are simply replacing N atoms in ZnPc with C−H or C−C$_6$H$_5$ units. ZnTBTrAP and ZnMPTBTrAP are obtained by replacing one nitrogen atom in ZnPc with C−H and C−C$_6$H$_5$, respectively. ZnTBP is obtained by replacing four nitrogen atoms in ZnPc with C−H units. ZnDPTB*trans*DAP is obtained by replacing two nitrogen atoms in ZnPc with C−C$_6$H$_5$ units.

The calculated absorption spectra for ZnTBTrAP, ZnTBP, ZnMPTBTrAP and ZnDPTB*trans*DAP in the first singlet excited state, together with the ESA of ZnPc (black solid line), are shown in Fig. 7. For molecules ZnTBTrAP and ZnMPTBTrAP, only one nitrogen atom in ZnPc is replaced by C−H and C−C$_6$H$_5$, respectively. The positions of the two absorption band peaks of ZnTBTrAP and ZnMPTBTrAP are closer compared with those of ZnPc. These two band peaks merge into one band peak for ZnTBP and ZnDPTB*trans*DAP. It is also noted that the absorptions of these modified ZnPc molecules for the transition energies between 2.0 eV and 2.5 eV are enhanced compared with that of ZnPc. Consequently, the absorption spectrum of ZnPc can be modified smoothly by replacing nitrogen atoms in ZnPc with C−H or C−C$_6$H$_5$. These observations may be utilized in the field of searching for enhanced optical limiting materials.[32] It should also be mentioned that the observed charge transfer characters of the transitions between the excited states for these modified ZnPc molecules are similar to those of ZnPc. Charge transfer also occurs between the edges and central parts
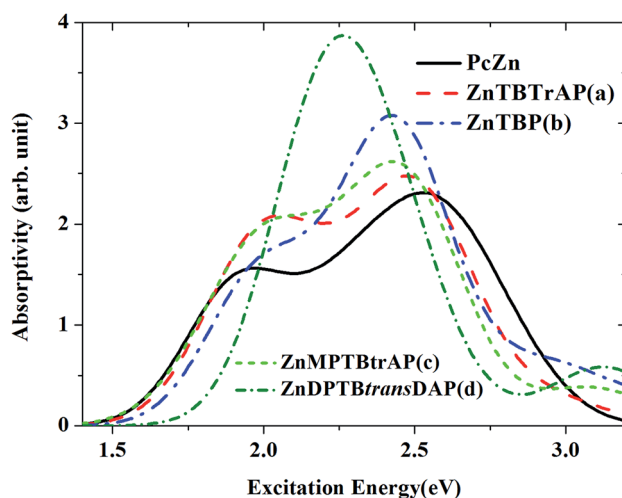

Fig. 7 Comparison of the absorption spectra of ZnPc and modified ZnPc in the first singlet excited state (S_1). The spectra are described using the calculated oscillator strengths and excitation energies broadened with the Gaussian function (FWHM = 0.4 eV).

of modified ZnPc. This is expected, as the structure of ZnPc is not totally destroyed with the present modifications.

C. First singlet excited state absorption of ZnPc dimers

It is well known that phthalocyanines in solution systems and doped in solid substrates possess aggregated states, such as dimers, which seriously affect the optical-limiting effect.[33] Here we investigated two configurations of ZnPc dimers. In one, the two ZnPc molecules are cofacially stacked. In the other configuration the two ZnPc molecules are cofacially stacked but with a slight shift. The distance between the two ZnPc molecules is fixed to 3.3 Å. Two ZnPc molecules are slipped 5.4 Å along the molecular axes in the second configuration. These configurations were reported by Yanagisawa *et al.*[25] Fig. 8 presents diagrams of these configurations. Top view (left side) and side view (right side) are both shown for these two configurations. In order to investigate the effect of molecular stacking on the absorption spectra, the ZnPc dimer structures are not optimized but the monomer geometry is optimized.

Fig. 9 shows the calculated absorption spectra for the ZnPc dimers with two different configurations in the first singlet excited state. For comparison, the absorption spectrum of the
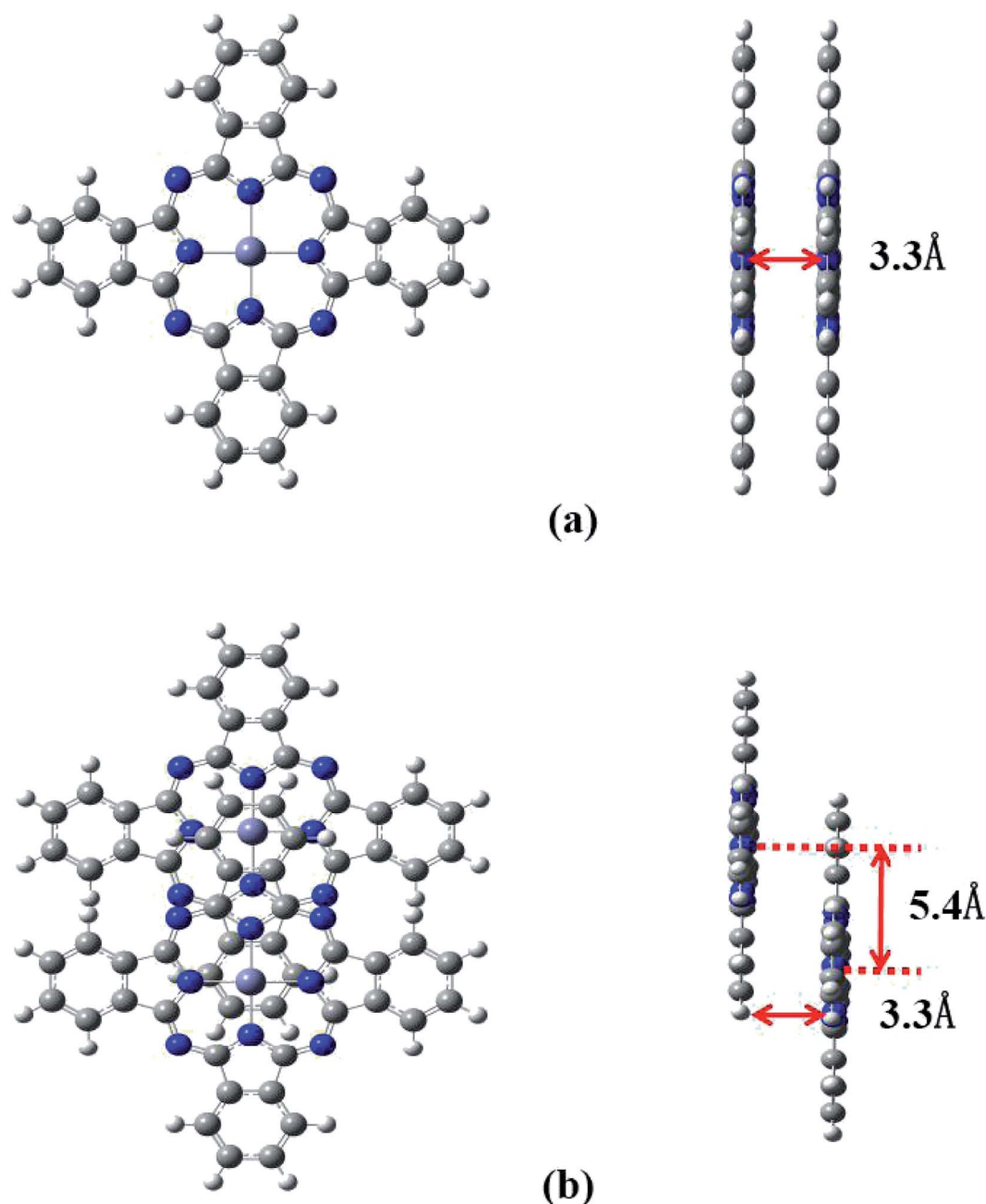

Fig. 8 Geometry of ZnPc dimers. White, grey and blue spheres represent hydrogen, carbon and nitrogen atoms, respectively (left: top view; right: side view). (a) Cofacially-stacked dimer, (b) slightly shifted cofacially-stacked dimer.
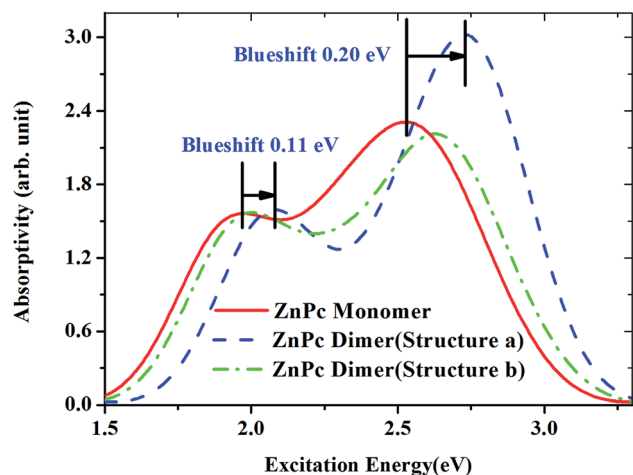
Fig. 9 Comparison of the absorption spectra of ZnPc and ZnPc dimers in the first singlet excited state (S$_1$). The spectra are described using the calculated oscillator strengths and excitation energies broadened with the Gaussian function (FWHM = 0.4 eV).

ZnPc monomer in the first singlet excited state is also included in Fig. 9 (red solid line). It is found that the band peaks of the ZnPc dimers are blueshifted compared with those of the ZnPc monomer. In addition, the blueshift depends on the geometrical overlap between the two ZnPc molecules. The ZnPc dimer with a complete overlapped configuration results in a larger blueshift compared with the configuration with partial overlap between the two monomers. Similar results were also observed by Yanagisawa *et al.* for ZnPc in the ground state.[25] It was shown that the absorption spectra of ZnPc dimers with configurations (a) and (b) in the ground state both result in blueshift. In addition, the blueshift of the absorption spectrum for the ZnPc dimer with configuration (a) in the ground state is also larger compared with that for configuration (b). This was attributed to the fact that configurations (a) and (b) are typical H-aggregates. Dipolar coupling between the two ZnPc molecules results in the blueshift of the absorption band.[34] The present paper shows that this is also true for the first singlet excited state absorption. According to Kasha's transition dipole–dipole interaction model, it means that the excitations for the first singlet excited state absorption bands may also come from the monomer transition dipoles being arranged side-by-side.[35]

IV. Conclusions

In the present paper, the absorption spectra of ZnPc, modified ZnPc and ZnPc dimers in the first singlet excited state were simulated. The predicted absorption band peaks for ZnPc are in excellent agreement with experimental measurements. It is shown that the S$_1$ → S$_3$ and S$_1$ → S$_{24}$ transitions, respectively, are the dominant contributions to the experimentally observed two band peaks. The excited states S$_1$ and S$_3$ can be well characterized by a single electronic transition from the highest occupied natural transition orbital (HONTO) to the lowest unoccupied natural transition orbital. In contrast, the dominant transitions for the higher excited state S$_{24}$ are HONTO →

LUNTO and HONTO−1 → LUNTO+1. The NTO analysis, together with the calculations of electron density difference between the two excitations, reveals that the transitions (S$_1$ → S$_3$ and S$_1$ → S$_{24}$) both show charge transfer character but with different charge transfer directions. It is also shown that the absorption of ZnPc in the first singlet excited state can be tuned through chemical modification of the nitrogen atoms in ZnPc. The calculated absorption spectra of ZnPc dimers indicate that the aggregation of ZnPc may result in a blueshift of the absorption. These observations are useful for tuning the optical-limiting window of ZnPc.

Conflicts of interest

There are no conflicts to declare.

Acknowledgements

References

1 M. Malinauskas, A. Zukauskas, S. Hasegawa, Y. Hayasaki, V. Mizeikis, R. Buividas and S. Juodkazis, *Light: Sci. Appl.*, 2016, **5**, e16133.
2 S. Perumbilavil, A. López-Ortega, G. K. Tiwari, J. Nogués, T. Endo and R. Philip, *Small*, 2018, **14**, 1701001.
3 S. Chen, W. H. Fang, L. Zhang and J. Zhang, *Angew. Chem., Int. Ed.*, 2018, **57**, 11252.
4 G. Zhao, Y. Feng, S. Guang, H. Xu, N. Li and X. Liu, *RSC Adv.*, 2017, **7**, 53785.
5 H. Xu, S. Q. Zhao, Y. Ren, W. Xu, D. B. Zhu, J. Z. Jiang and J. F. Cai, *RSC Adv.*, 2016, **6**, 21067.
6 S. A. Fischer, C. J. Cramer and N. Govind, *J. Phys. Chem. Lett.*, 2016, **7**, 1387.
7 R. B. Roseli, P. C. Tapping and T. W. Kee, *J. Phys. Chem. Lett.*, 2017, **8**, 2806.
8 Y. Bai, J. H. Olivier, H. Yoo, N. F. Polizzi, J. Park, J. Rawson and M. J. Therien, *J. Am. Chem. Soc.*, 2017, **139**, 16946.
9 E. F. Oliveira, J. Shi, F. C. Lavarda, L. Luer, B. Milian-Medina and J. Gierschner, *J. Chem. Phys.*, 2017, **147**, 034903.
10 S. Ling, S. Schumacher, I. Galbraith and M. J. Paterson, *J. Phys. Chem. C*, 2013, **117**, 6889.
11 B. Q. Liu, L. Wang, D. Y. Gao, J. H. Zou, H. L. Ning, J. B. Peng and Y. Cao, *Light: Sci. Appl.*, 2016, **5**, e16137.
12 Z. Li, H. Li, B. J. Gifford, W. D. N. Peiris, S. Kilina and W. Sun, *RSC Adv.*, 2016, **6**, 41214.

13 J. Savolainen, D. van der Linden, N. Dijkhuizen and J. L. Herek, *J. Photochem. Photobiol., A*, 2008, **196**, 99.

14 D. R. Tackley, G. Dent and W. E. Smith, *Phys. Chem. Chem. Phys.*, 2001, **3**, 1419.

15 N. Marom, O. Hod, G. E. Scuseria and L. Kronik, *J. Chem. Phys.*, 2008, **128**, 164107.

16 M. S. Liao and S. Scheiner, *J. Chem. Phys.*, 2001, **114**, 9780.

17 P. N. Day, Z. Wang and R. Pachter, *J. Mol. Struct.: THEOCHEM*, 1998, **455**, 33.

18 J. Ahlund, K. Nilson, J. Schiessling, L. Kjeldgaard, S. Berner, N. Martensson, C. Puglia, B. Brena, M. Nyberg and Y. Luo, *J. Chem. Phys.*, 2006, **125**, 034709.

19 S. Ahmadi, M. N. Shariati, S. Yu and M. Gothelid, *J. Chem. Phys.*, 2012, **137**, 084705.

20 T. C. VanCott, J. L. Rose, G. C. Misener, B. E. Williamson, A. E. Schrimpf, M. E. Boyle and P. N. Schatz, *J. Phys. Chem.*, 1989, **93**, 2999.

21 D. A. Fernández, J. Awruch and L. E. Dicelio, *Photochem. Photobiol.*, 1996, **63**, 784.

22 D. S. Lawrence and D. G. Whitten, *Photochem. Photobiol.*, 1996, **64**, 923.

23 G. Ricciardi, A. Rosa and E. J. Baerends, *J. Phys. Chem. A*, 2001, **105**, 5242.

24 R. F. Theisen, L. Huang, T. Fleetham, J. B. Adams and J. Li, *J. Chem. Phys.*, 2015, **142**, 094310.

25 S. Yanagisawa, T. Yasuda, K. Inagaki, Y. Morikawa, K. Manseki and S. Yanagida, *J. Phys. Chem. A*, 2013, **117**, 11246.

26 L. T. Ueno, A. E. H. Machado and F. B. C. Machado, *J. Mol. Struct.: THEOCHEM*, 2009, **899**, 71.

27 X. Sheng, H. Zhu, K. Yin, J. Chao, J. Wang, C. Wang, J. Shao and F. Chen, *J. Phys. Chem. C*, 2020, **124**, 4693.

28 M. J. Frisch, G. W. Trucks, H. B. Schlegel, G. E. Scuseria, M. A. Robb, J. R. Cheeseman, G. Scalmani, V. Barone, B. Mennucci, G. A. Petersson, H. Nakatsuji, M. Caricato, X. Li, H. P. Hratchian, A. F. Izmaylov, J. Bloino, G. Zheng, J. L. Sonnenberg, M. Hada, M. Ehara, K. Toyota, R. Fukuda, J. Hasegawa, M. Ishida, T. Nakajima, Y. Honda, O. Kitao, H. Nakai, T. Vreven, J. A. Montgomery Jr, J. E. Peralta, F. Ogliaro, M. Bearpark, J. J. Heyd, E. Brothers, K. N. Kudin, V. N. Staroverov, R. Kobayashi, J. Normand, K. Raghavachari, A. Rendell, J. C. Burant, S. S. Iyengar, J. Tomasi, M. Cossi, N. Rega, J. M. Millam, M. Klene, J. E. Knox, J. B. Cross, V. Bakken, C. Adamo, J. Jaramillo, R. Gomperts, R. E. Stratmann, O. Yazyev, A. J. Austin, R. Cammi, C. Pomelli, J. W. Ochterski, R. L. Martin, K. Morokuma, V. G. Zakrzewski, G. A. Voth, P. Salvador, J. J. Dannenberg, S. Dapprich, A. D. Daniels, O. Farkas, J. B. Foresman, J. V. Ortiz, J. Cioslowski, and D. J. Fox, *Gaussian 09, Revision D.01*, Gaussian, Inc., Wallingford, CT, 2009.

29 M. W. Schmidt, K. K. Baldridge, J. A. Boatz, S. T. Elbert, M. S. Gordon, J. H. Jensen, S. Kosekt, N. Matsunaga, K. A. Nguyen, S. J. Su, T. L. Windus, M. Dupuis and J. A. Montgomery, *J. Comput. Chem.*, 1993, **14**, 1347.

30 T. Lu and F. Chen, *J. Comput. Chem.*, 2012, **33**, 580.

31 D. N. Bowman, J. C. Asher, S. A. Fischer, C. J. Cramer and N. Govind, *Phys. Chem. Chem. Phys.*, 2017, **19**, 27452.

32 N. Nwaji, J. Mack and T. Nyokong, *New J. Chem.*, 2017, **41**, 14351.

33 J. Chen, Y. Xu, M. Cao, Y. Wang, T. Liang, H. Li, S. Wang and G. Yang, *J. Mater. Chem. C*, 2018, **6**, 9767.

34 N. C. Maiti, S. Mazumdar and N. Periasamy, *J. Phys. Chem. B*, 1998, **102**, 1528.

35 M. Kasha, *Radiat. Res.*, 1963, **20**, 55.